

The effect of temperature anisotropy on observations of Doppler dimming and pumping in the inner corona

Xing Li^{1,2}, Shadia Rifai Habbal¹, John Kohl¹ and Giancarlo Noci³

¹Harvard-Smithsonian Center for Astrophysics, Cambridge, MA 02138, USA

²Department of Earth and Space Sciences, University of Science and Technology of China, Hefei, Anhui 230026, China

³Universita di Firenze, I-2025 Firenze, Italy

ABSTRACT

Recent observations of the spectral line profiles and intensity ratio of the O VI 1032 Å and 1037.6 Å doublet by the Ultraviolet Coronagraph Spectrometer (UVCS) on the Solar and Heliospheric Observatory (SOHO), made in coronal holes below 3.5 R_s , provide evidence for Doppler dimming of the O VI 1037.6 Å line and pumping by the chromospheric C II 1037.0182 Å line. Evidence for a significant kinetic temperature anisotropy of O⁵⁺ ions was also derived from these observations. We show in this Letter how the component of the kinetic temperature in the direction perpendicular to the magnetic field, for both isotropic and anisotropic temperature distributions, affects both the amount of Doppler dimming and pumping. Taking this component into account, we further show that the observation that the O VI doublet intensity ratio is less than unity can be accounted for only if pumping by C II 1036.3367 Å in addition to C II 1037.0182 Å is in effect. The inclusion of the C II 1036.3367 Å pumping implies that the speed of the O⁵⁺ ions can reach 400 km/s around 3 R_s which is significantly higher than the reported UVCS values for atomic hydrogen in polar coronal holes. These results imply that oxygen ions flow much faster than protons at that heliocentric distance.

Subject headings: solar wind — Sun: corona — Sun: UV radiation

1. Introduction

The Ultraviolet Coronagraph Spectrometer (UVCS) on SOHO has proven to be a powerful tool for probing the physical conditions in the inner corona (Kohl et al. 1995, 1997, 1998; Habbal et al. 1997; Noci et al. 1997). These ultraviolet measurements extend to at least 3.5 R_s in polar coronal holes, and to 10 R_s in denser coronal plasmas such as streamers. As described by Kohl & Withbroe (1982), and Withbroe et al. (1982), determinations of proton and heavy ion flow speeds in the inner corona can be made using the Doppler dimming effect (see Hyder & Lites 1970). This method is applicable when ultraviolet coronal lines are formed primarily by the resonance scattering of ions by the chromospheric or transition region radiation in the same wavelength range, in addition to collisional excitation. As ions flow outwards in the corona, the fraction of the spectral line formed by resonance scattering becomes Doppler-shifted out of resonance with the disk emission. Subsequently, only the collisional component then remains. Of particular interest is the application of this technique to doublets such as the O VI 1032 and 1037.6 Å lines. In a static corona, the ratio of the line intensities 1032/1037.6 equals 4 when resonant scattering is dominant, and reduces to 2 when collisional excitation only is present.

Extending the concept of the Doppler dimming effect, Noci et al. (1987) showed that determinations of flow speeds in the range of 100 to 250 km/s could also be made. With the assumption of isotropic kinetic temperatures, that study was based on the possibility of scattering of the C II 1037.0 Å line by the coronal O⁵⁺ ions when the ion flow speed is in the range of 100 to 250 km/s. When this occurs, the ratio 1032/1037.6 of the two line intensities is then expected to reach a minimum as the flow speed of the ions increases as a function of heliocentric distance.

Another important discovery from UVCS is the observation of broader than expected profiles of O VI 1032 and 1037.6 Å lines in polar coronal holes. Since these profiles are measured along the line of sight which is perpendicular to the radial direction at the point of closest approach to the Sun, their widths yield a measure of the O⁵⁺ kinetic temperature in the direction approximately perpendicular to the magnetic field. UVCS observations also revealed that the O VI 1032/1037.6 intensity ratio reached a value of less than one at about 2.5 R_s in coronal holes. If the kinetic temperatures parallel to the magnetic field were similar to the observed perpendicular temperatures, the O VI intensity ratio could not reach a value near unity. Hence, observations of broad line profiles and a decrease in the line ratios below a value of one led Kohl et al. (1997) to conclude that a significant kinetic temperature anisotropy exists for coronal O⁵⁺ at a heliocentric distance of about 2.5 R_s .

Motivated by the UVCS observations, we illustrate in this Letter how the component of the kinetic temperature along the line of sight, for both isotropic and anisotropic temperature distributions, affect the derivations of outflow velocities from the O VI intensity ratio. However, by extending the effect of Doppler dimming and pumping of the O VI 1037.6 Å line to include another almost equally strong chromospheric C II 1036.3367 Å line in the vicinity of the C II 1037.0182 Å line (Warren et al. 1997), we show that the pumping by both C II lines can account for the O VI line intensity ratios recently observed by UVCS (Kohl et al. 1997).

2. Effect of temperature anisotropy on Doppler dimming and pumping

The resonant scattering component of a spectral line, $I_R(\nu)$, integrated along a line of sight (LOS) chosen along the x -axis can be written as (Kohl & Withbroe, 1982):

$$\begin{aligned}
 I_R(\nu) = & \frac{hB_{12}}{4\pi\nu_0} \int_{-\infty}^{\infty} n_i dx \int_{\omega} [a + b(\mathbf{n} \cdot \mathbf{n}')^2] d\omega \times \\
 & \int_{-\infty}^{\infty} I(\nu', \omega) d\nu' \int_{-\infty}^{\infty} f(\mathbf{v}) \delta\left(\nu' - \nu_0 - \frac{\nu_0}{c} \mathbf{v} \cdot \mathbf{n}'\right) \\
 & \times \delta\left(\nu_0 - \nu + \frac{\nu_0}{c} \mathbf{v} \cdot \mathbf{n}\right) d\mathbf{v}, \tag{1}
 \end{aligned}$$

where B_{12} is the Einstein coefficient, h is Planck's constant, $I(\nu', \omega)$ is the intensity of the chromospheric radiation at wave frequency ν' . The only photons that can be scattered by an ion, O⁵⁺ in the example considered here, with a velocity \mathbf{v} , are those with $\nu' = \nu_0 + (\nu_0/c)\mathbf{v} \cdot \mathbf{n}'$ where ν_0 is the central wave frequency of the oxygen spectral lines and \mathbf{n}' is the vector describing the direction of the incident chromospheric radiation. n_i is the number density of O⁵⁺, $\mathbf{v} \cdot \mathbf{n}$ is equal to v_x , ω is the angular direction, and $f(\mathbf{v})$ is the velocity distribution function describing the oxygen ions. $[a + b(\mathbf{n} \cdot \mathbf{n}')^2]$ is the angular dependence of the scattering process for the oxygen lines. For O VI 1032 Å, a is equal to 7/8 and b is equal to 3/8; for O VI 1037.6 Å, a is 1 and b is 0 (Noci et al. 1987).

If a bi-Maxwellian velocity distribution is assumed, the integral over \mathbf{v} can be computed analytically to yield an expression for $I_R(\nu)$ which can then be integrated numerically over x , ω , and ν' . As an illustration, we define a rectangular coordinate system with the $+x$ -axis pointing towards the observer along the LOS (see Figure 1). At any point along the LOS, the $+z$ -axis is chosen to point towards the Sun and to be perpendicular to the LOS in the plane formed by the LOS and Sun center O. The three angles, Φ , θ and Ψ , defined in this coordinate system are shown in Figure 1.

For a bi-Maxwellian velocity distribution, $f(\mathbf{v})$ can be written as

$$f(\mathbf{v}) = \left(\frac{m}{2\pi k T_{\parallel}} \right)^{1/2} \left(\frac{m}{2\pi k T_{\perp}} \right) \exp \left(\frac{-m}{2k T_{\parallel}} (v_{\parallel} - u)^2 \right) \times \exp \left(\frac{-m}{2k T_{\perp}} v_{\perp}^2 \right) \quad (2)$$

where u is the bulk outflow velocity along the radial direction, T_{\parallel} and T_{\perp} are the kinetic temperatures in the radial and perpendicular to radial directions with the assumption that the magnetic field expands radially.

We define

$$\alpha_{\parallel} = \frac{2k T_{\parallel}}{m}, \quad \alpha_{\perp} = \frac{2k T_{\perp}}{m}, \quad (3)$$

The last integration in (1):

$$F = \int_{-\infty}^{\infty} f(\mathbf{v}) \delta \left(\nu' - \nu_0 - \frac{\nu_0}{c} \mathbf{v} \cdot \mathbf{n}' \right) \times \delta \left(\nu_0 - \nu + \frac{\nu_0}{c} \mathbf{v} \cdot \mathbf{n} \right) d\mathbf{v}$$

can then be transformed into the analytical expression:

$$F = \frac{A^{-1/2}}{\pi \sqrt{\alpha_{\parallel} \alpha_{\perp}}} \exp \left(-\frac{1}{\alpha_{\parallel}} \left[\beta_1 \sin \psi - u + \frac{\beta_2 d_z \cos \psi}{d_y^2 + d_z^2} \right]^2 \right) \exp \left(-\frac{1}{\alpha_{\perp}} \left[\beta_1 \cos \psi - \frac{\beta_2 d_z \sin \psi}{d_y^2 + d_z^2} \right]^2 - \frac{\beta_2^2 d_y^2}{\alpha_{\perp} (d_y^2 + d_z^2)} + \Delta \right) \quad (4)$$

where

$$\Delta = \frac{d_y^2 \cos^2 \psi}{\alpha_{\parallel}^2 \alpha_{\perp}^2 A} \left[\frac{\beta_2 d_z \cos \psi (\alpha_{\perp} - \alpha_{\parallel})}{d_y^2 + d_z^2} + \alpha_{\perp} (\beta_1 \sin \psi - u) - \alpha_{\parallel} \beta_1 \sin \psi \right]^2 \quad (5)$$

d_x , d_y , and d_z come from $\mathbf{v} \cdot \mathbf{n}' = v_x d_x + v_y d_y + v_z d_z$, and are given by

$$\begin{aligned} d_x &= -\sin \phi \cos \theta \cos \psi + \cos \phi \sin \psi, \\ d_y &= -\sin \phi \sin \theta, \\ d_z &= -\cos \phi \cos \psi - \sin \phi \cos \theta \sin \psi \end{aligned} \quad (6)$$

and

$$\begin{aligned} A &= \frac{d_z^2}{\alpha_{\perp}} + d_y^2 \left(\frac{\cos^2 \psi}{\alpha_{\parallel}} + \frac{\sin^2 \psi}{\alpha_{\perp}} \right), \\ \beta_1 &= \frac{c}{\nu_0} (\nu - \nu_0), \quad \beta_2 = \frac{c}{\nu_0} [(\nu_0 - \nu') - d_x (\nu_0 - \nu)] \end{aligned} \quad (7)$$

Inspection of (1) and (4) shows that the measured intensity of the resonantly scattered component, $I_R(\nu)$, depends on the physical properties of the oxygen ions and the strength of the chromospheric radiation. Since the velocity distribution perpendicular to the radial direction will have a component along the direction of the incident radiation from the whole solar disk (except from Sun center), T_\perp will also contribute to the resonance scattering. Consequently, the resonantly scattered component of the oxygen lines along the line of sight results from the combined effects of disk radiation, T_\perp and T_\parallel , Doppler dimming and pumping, leading to ratios similar to those shown in Figure 2.

Figure 2a shows the intensity ratio 1032/1037.6 as a function of O^{5+} outflow velocity obtained by computing the integral along the LOS at $3 R_s$ of both the resonantly scattered component given in (1) and the collisionally excited component (see, for example, expression given by Withbroe et al. 1982). In this example, the electron density is taken to be $4.7 \times 10^4 \text{ cm}^{-3}$ at $3 R_s$, which is at the upper limit of the electron density profile derived from polarization brightness measurements at that distance (Fisher and Guhathakurta, 1995). The intensity of the disk radiation used, $I_{OVI}(1032) = 305$, $I_{OVI}(1037.6) = 152.5$, and $I_{CII}(1037) = 52 \text{ erg cm}^{-2} \text{ s}^{-1} \text{ sr}^{-1}$, and the $1/e$ half width of 0.1 and 0.07 Å for the O VI and C II lines respectively, were those given by Noci et al. (1987). The ratio of the C II and O VI line intensities is also consistent with the more recent values given by Warren et al. (1997). Contributions to the LOS from larger heliocentric distances are estimated using that density profile, assuming spherical symmetry, and a corresponding velocity inferred from the constancy of mass flux. The electron temperature is kept constant at 10^6 K. The parallel and perpendicular temperatures of the O^{5+} ions are kept constant along the LOS. Different combinations of parallel and perpendicular temperatures, including isotropic and anisotropic temperatures, were chosen to produce the curves shown in Figure 2a. The values are within the range expected from UVCS observations (see Kohl et al., 1997). The 1032/1037.6 line ratios thus computed include the pumping of the O VI 1037.6 Å line by C II 1037 Å. The calculated ratio is found to be insensitive to the electron temperature or to the elemental abundance.

For an anisotropic kinetic temperature distribution, Figure 2a clearly shows how the ratio cannot be smaller than 1 if the perpendicular kinetic temperature is as high as 2.5×10^8 K, as implied by the UVCS observations (see Kohl et al. 1997). At such a high perpendicular kinetic temperature, the projection of the perpendicular velocity distribution on the incident light rays is strong enough that it broadens the spectral width of the C II 1037.018 Å pumping, so that the pumping by that line alone could only account for a ratio of 1 or larger. The minimum value of the O VI 1032/1037 ratio in the examples of anisotropic temperatures in Figure 2a is ≥ 1 even when the parallel temperature is as low as 10^5 K.

However, UVCS observations in polar coronal holes yield a ratio of 0.8 at $2.5 R_s$ and 0.7 at $3 R_s$ (see Kohl et al. 1997). Interestingly, observations by SUMER (Feldman et al. 1997, Curdt et al. 1997, Warren et al. 1997) and UVCS show that there is another C II 1036.3 Å line which is almost as strong as the C II 1037 Å line. In optically thin conditions, the intensity ratio between the C II 1036.3 and C II 1037 lines is 0.5 (e.g., Verner et al. 1996). However, the C II lines are emitted from the chromosphere and are probably not optically thin. Indeed, Sun center disk observations by Warren et al. (1997) yield a ratio of 0.84, while Curdt et al. (1997) measured a ratio of 0.93 in a field of view encompassing disk and some coronal emission in a polar coronal hole. Given that the resonance scattering in the corona is due to the disk emission, we adopt the ratio C II 1036.3/1037 of 0.84 given by Warren et al. (1997) in our calculations.

The additional pumping by this second line is maximum when the O^{5+} velocity reaches 370 km/s. As shown in Figure 2b, if the pumping of both the C II 1037 and 1036.3 Å lines is included, the profile of the O VI 1032/1037 line ratio becomes very different. For the examples of isotropic temperatures (thin solid and dotted lines), the O VI 1032/1037 ratio has two minima reflecting the pumping by the two C II

lines respectively. However, in the presence of anisotropy the two minima merge into a broad one at 370 km/s. The ratio rises back to a value of 2 at 600 km/s, as resonance scattering disappears and collisional excitation only remains.

We also note that when pumping by only one C II line is considered, the different curves in Figure 2a intersect at a common value of 80 km/s for a ratio of 2.6. When pumping by both lines is taken into account (Figure 2b), the curves still intersect at this value, but also around 400 km/s for a ratio of 1. Hence, these examples illustrate that the theoretical value of 2 for the ratio corresponding to 94 km/s and an isotropic temperature of 1.6×10^6 K (Noci et al. 1987), is now slightly shifted to a higher ratio and a lower flow speed when the contribution of the perpendicular temperature is taken into account in the line of sight integration.

The effect of the pumping by the two C II lines can also be explored using a self-consistent multifluid solar wind model (Li et al. 1997) with heating by MHD turbulence (Kraichnan 1965, Li et al. 1998). The results shown in Figure 3 are plotted out to $10 R_s$ for comparison with UVCS observations, even though the computations are carried out to 1 AU. The density of the oxygen ions at the coronal base is chosen such that the line intensities fit the observed ones there. The density profile matches that inferred from polarization brightness measurements in the inner corona (see Fisher and Guhathakurta, 1995), and the derived proton velocity of 740 km/s and mass flux of $1.96 \times 10^8 \text{ cm}^{-2}$ at 1 AU match observational constraints (e.g. Phillips et al. 1995). It is seen from Figure 3a,3b that this mechanism can lead to a significant anisotropy in the inner corona, and that the flow speed of the oxygen ions exceeds that of protons there. The corresponding widths and intensity ratio 1032/1037 are shown in Figure 3c,3d. Because of the consecutive pumping by the two C II lines, the resonantly scattered component of O VI 1037.6 Å will be enhanced at two discrete values, leading to a reduction in the width of the O VI 1037.6 Å line, which occurs approximately at 2.25 and 3.25 R_s in this model. As a result, the O VI 1037.6 Å line will be narrower than the O VI 1032 Å line. As shown in Figure 3d, the pumping by the C II 1036.3 Å line can strongly influence the intensity ratio 1032/1037.6. When this pumping is neglected (dotted line) the ratio becomes significantly larger than 1, but drops below 1, as observed (see Kohl et al. 1997a, 1997b), when the effect is included.

3. Conclusions

This study demonstrates that the anisotropic kinetic temperatures of O^{5+} implied by UVCS observations (Kohl et al. 1997) in the inner corona can significantly affect the Doppler dimming and pumping, and subsequently increase the observed O VI 1032/1037.6 line ratio expected for a given velocity. Another aspect of this study is that the pumping by both the C II 1037.018 Å and a second C II line at 1036.3 Å is necessary to account for the observed intensity ratios. The inclusion of this second C II line, however, implies that the O^{5+} ions can reach speeds of 400 km/s near $3 R_s$. Consequently, the diagnostic techniques used in UVCS observations can be extended to much higher flow speeds than originally expected.

We also note that protons, which are strongly coupled to the neutral hydrogen, are expected to have the same flow speed as the neutrals (see Olsen et al. 1994, Allen et al. 1998). Hence, based on the recent UVCS observations, this study, together with the empirical model results by Kohl et al. (1998), shows that the O^{5+} ions are flowing significantly faster than the protons around $3 R_s$ in the fast solar wind. This is an indication that whatever mechanism is responsible for coronal heating and solar wind acceleration must preferentially accelerate minor ions such that they can flow faster than protons in the inner corona.

The results presented in this Letter were motivated by the recent UVCS observations. We extend our thanks to the UVCS team for the outstanding value of their measurements. We gratefully acknowledge helpful discussions with Drs. N. S. Brickhouse, S. Cranmer, J. C. Raymond, and L. Strachan, and thank M. Romoli for pointing out to us a correction to Equation (1) as it appeared in an earlier version of the manuscript. UVCS is supported by the National Aeronautics and Space Administration under grant NAG5-3192 to the Smithsonian Astrophysical Observatory, by Agenzia Spaziale Italiana, and by Swiss funding agencies. X. Li and S. R. Habbal were supported by NASA grants NA65-6271 and NA65-6215 to the Smithsonian Astrophysical Observatory. X. Li was also supported by a predoctoral fellowship from the Smithsonian Astrophysical Observatory.

4. References

- Allen, L., Habbal, S.R., and Hu, Y.-Q. 1998, JGR, in press
- Curdt, W., et al., 1997 A&AS, 126, 281
- Feldman, U., et al. 1997, ApJS, 113, 195
- Fisher, R.R. and Guhathakurta, M. 1995, ApJ, 447, L139
- Habbal, S.R., et al. 1997, ApJ, 489, L103
- Hyder, C.L. & Lites, B.W. 1970, Sol. Phys., 14, 147
- Kohl, J.L. & Withbroe, G.L. 1982, ApJ, 256, 263
- Kohl, J.L. et al. 1995, Sol. Phys., 162, 313
- Kohl, J.L. et al. 1997, Sol. Phys., 175, 613
- Kohl, J. L. et al. 1998, ApJ (this issue)
- Kraichnan, R. 1965, Phys. Fluids, 8, 1385
- Li, X., Esser, R., Habbal, S.R. & Hu, Y.-Q. 1997, J. Geophys. Res., 102, 17419
- Li, X., Habbal, S.R., Esser, R., & Hollweg, J. V. 1998 (in preparation)
- Noci, G., Kohl, J.L. & Withbroe, G.L. 1987, ApJ, 315, 706
- Noci, G. et al. 1997, ASP Conference Series, in press
- Olsen, E.L., Leer, E., Holzer, T.E. 1994, ApJ, 420, 913
- Phillips, J. L., et al., 1995, Science, 268, 1030
- Verner, D.A., Verner, E.M., Ferland, G.J. 1996, Atomic Data and Nuclear Data Tables, 61, 1
- Warren, H.P., Mariska, J.T., Wilhelm, K., and Lemaire, P. 1997, ApJ, 484, L91
- Withbroe, G.L., Kohl, J.L., Weiser, H., & Munro, R.H. 1982, Space Sci. Rev., 33, 17

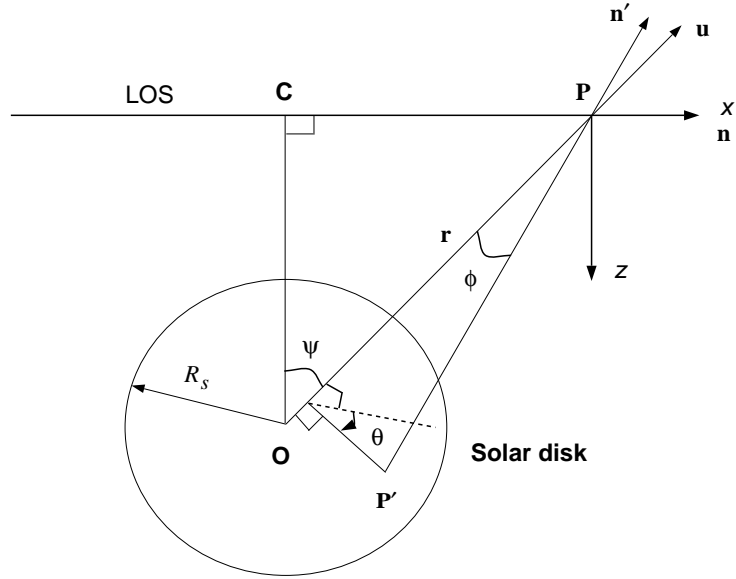


Fig. 1.— Coordinate system used to derive Equation (5). LOS is the line of sight chosen along the x-axis. C represents the point of closest approach from the LOS to the Sun. P is a point along the LOS which contributes to the integral in (1). T_{\parallel} is the component of the kinetic temperature along the radial direction \mathbf{r} . \mathbf{r} is also the direction of the outflow velocity \mathbf{u} . T_{\perp} is the component of the kinetic temperature in a plane perpendicular to \mathbf{r} at P. P' is a point on the solar disk from which the radiation is emitted. θ is the angle between the x-z plane and the plane OPP' . The projection of P' onto that plane is shown by the dashed line. The direction of the radiation from P' reaching P is indicated by the unit vector \mathbf{n}' .

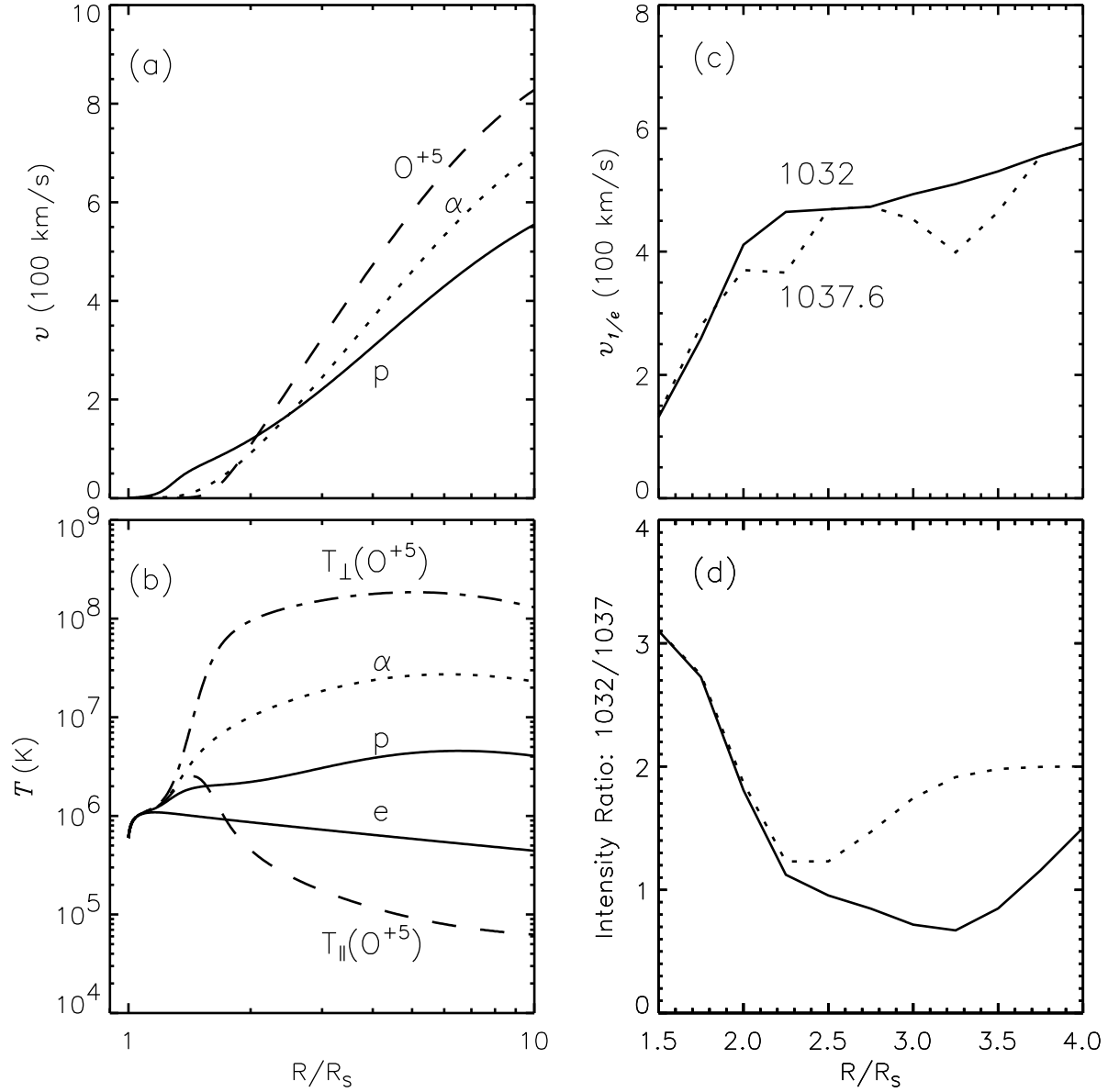


Fig. 3.— Multi-fluid solar wind model computations for electron/protons, alpha particles and oxygen ions: (a) flow speeds, (b) temperature of species, (c) line widths, $v_{1/e}$, and (d) intensity ratio. In (d) the dotted line corresponds to pumping by only C II 1037.0 Å, while the solid line includes the pumping by both C II 1037.0 and 1036.3 Å lines.